Distinct roles for Khd1p in the localization and expression of bud-localized mRNAs in yeast

YUKO HASEGAWA,[1,2] KENJI IRIE,[1,2] and ANDRÉ P. GERBER[3]

[1]Department of Molecular Cell Biology, Graduate School of Comprehensive Human Sciences, University of Tsukuba, 305-8575 Tsukuba, Japan
[2]Institute of Basic Medical Sciences, University of Tsukuba, 305-8575 Tsukuba, Japan
[3]Institute of Pharmaceutical Sciences, ETH Zurich, 8093 Zurich, Switzerland

ABSTRACT

The RNA-binding protein Khd1p (KH-domain protein 1) is required for efficient localization of *ASH1* mRNA to the bud-tip, probably acting as a translational repressor during mRNA transport in yeast. Here, we have systematically examined Khd1p mRNA targets and colocalization with known bud-tip-localized mRNAs in vivo. Affinity purification and DNA microarray analysis of Khd1p-associated mRNAs revealed hundreds of potential mRNAs targets, many of them encoding membrane-associated proteins. The putative targets include the messages for *MID2, MTL1, WSC2, SRL1, EGT2, CLB2, ASH1*, and Khd1p colocalizes with these mRNAs at the bud-tip. The combination of bioinformatics, RNA localization, and in vitro RNA-binding assays revealed that Khd1p binds to CNN repeats in coding regions of mRNA targets. Among the proteins encoded by previously known bud-tip-localized mRNAs, only Mtl1p levels were decreased in *khd1*Δ mutant cells, whereas Ash1p and Srl1p were reduced in cells overexpressing *KHD1*. Hence, Khd1p differentially affects gene expression possibly due to combinatorial arrangement with additional factors reflecting the redundant structure of post-transcriptional regulatory systems.

Keywords: mRNA localization; RNA-binding protein; KHD1; translation; mRNA stability; yeast

INTRODUCTION

The asymmetric distribution of proteins is of vital importance for cellular function and cell fate determination. mRNA localization is a widespread mechanism for achieving asymmetric distribution of proteins. In embryos, mRNA localization is utilized for morphogen gradient formation and for the asymmetric distribution of cell fate determinants. In somatic cells, mRNA localization is utilized for protein targeting to the specific regions where they are required. Localized mRNAs are generally characterized by *cis*-acting localization element(s), so called zipcodes, which are often found in the 3′-untranslated region (3′-UTR) and interact with specific RNA-binding proteins (RBPs), forming large ribonucleoprotein (RNP) complexes. The RNP complex is transported by motor proteins along actin or microtubule filaments to particular cell destinations (Tekotte and Davis 2002; López de Heredia and Jansen 2004; St Johnston 2005; Czaplinski and Singer 2006; Du et al. 2007).

Reprint requests to: Kenji Irie, Department of Molecular Cell Biology, Graduate School of Comprehensive Human Sciences, University of Tsukuba, 1-1-1 Tennoudai, Tsukuba, 305-8575, Japan; e-mail: kirie@md.tsukuba.ac.jp; fax: 81-29-853-3066.

Article published online ahead of print. Article and publication date are at http://www.rnajournal.org/cgi/doi/10.1261/rna.1016508.

A well-studied example for actin-dependent RNA transport concerns *ASH1* mRNA localization to the bud-tip of dividing yeast cells (Gonsalvez et al. 2005; Müller et al. 2007). *ASH1* encodes a transcriptional repressor for HO endonuclease and thus prevents mating type switching in daughter cells (Bobola et al. 1996; Sil and Herskowitz 1996). *ASH1* mRNA transport involves five *SHE* genes (Jansen et al. 1996; Long et al. 1997; Takizawa et al. 1997): *SHE1/MYO4* encodes a type V myosin motor that mediates *ASH1* mRNA transport along actin cables (Haarer et al. 1994, Bertrand et al. 1998; Munchow et al. 1999; Takizawa and Vale 2000). *SHE2* encodes an mRNA-binding protein that associates with Myo4p through an adaptor protein, which is encoded by *SHE3* (Munchow et al. 1999; Takizawa and Vale 2000). She2p directly binds to *cis*-acting elements in *ASH1* mRNA that are sufficient to localize RNA to the bud (Bohl et al. 2000; Long et al. 2000; Niessing et al. 2004; Jambhekar et al. 2005; Olivier et al. 2005). Hence, RNA and She2-She3-Myo4 proteins form a RNP complex called ''locasome'' that travels along actin cables to the bud-tip. The molecular involvement of two other *SHE* genes, *SHE4*, encoding a protein involved in actin-dependent endocytosis, and *SHE5* coding for a formin ortholog involved in actin regulation (Wendland et al. 1996; Evangelista et al. 1997) have not been clearly resolved yet.

Beside *ASH1*, a genome-wide screen revealed at least 23 additional mRNAs that are also transported by the locasome to the bud-tip of daughter cells (Takizawa et al. 2000; Shepard et al. 2003; Andoh et al. 2006). These mRNAs encode a variety of proteins, several involved in stress responses and cell wall maintenance. On the other hand, several RNA-binding proteins have been found to regulate *ASH1* mRNA transport and translation (Long et al. 2001; Irie et al. 2002; Gu et al. 2004). Among them, KH-domain protein 1 (Khd1p) has been shown to bind *ASH1* mRNA and is required for efficient localization of the mRNA (Irie et al. 2002). Overexpression of Khd1p decreased the level of Ash1 protein, suggesting that Khd1p represses translation of *ASH1* mRNA during transport to the bud-tip (Irie et al. 2002). Moreover, repression of *ASH1* mRNA translation by Khd1p can be released at the distal tips through phosphorylation of Khd1p by the casein kinase Yck1p (Paquin et al. 2007). However, beside *ASH1*, the mRNA targets for Khd1p are unknown and it is not clear whether Khd1p is required for proper localization and translation of other bud-tip-localized mRNAs. Khd1p contains three K homology (KH) RNA-binding domains, and its feature is similar to mammalian heterogeneous nuclear RNP K (hnRNP K) and poly(C)-binding proteins (PCBP1-4) (Makeyev and Liebhaber 2002; Bomsztyk et al. 2004). Khd1p, also called Hek2p (heterogenoeous nuclear RNP K-like gene), has also been reported to be involved in the structural and functional organization of telomeric chromatin (Denisenko and Bomsztyk 2002), but it remains unknown how Khd1p/Hek2p regulates them.

Here, we have systematically identified Khd1p RNA targets with DNA microarrays, and we examined Khd1p colocalization with bud-tip-localized mRNAs in vivo. Khd1p binds hundreds of mRNAs, including a subset of the 24 known bud-tip-localized mRNAs to which Khd1p colocalizes at the bud tip. Through the combination of bioinformatics, RNA localization, and in vitro RNA-binding assays, we show that Khd1p binds to (CNN) repeats in the coding regions of mRNA targets. Examination of protein levels of the bud-localized mRNAs targeted by Khd1p showed that the amount of Ash1 and Srl1 proteins are decreased in cells overexpressing *KHD1*, whereas Mtl1 protein was decreased in the *khd1Δ* mutant, suggesting that Khd1p positively and negatively regulates gene expression possibly through combinatorial arrangement with other RBPs.

RESULTS

Genome-wide identification of mRNAs associated with Khd1p

To identify RNAs associated with Khd1p, we applied tandem-affinity purification (TAP) of tagged Khd1p, followed by the analysis of bound RNAs with DNA microarrays (Gerber et al. 2004). Cells expressing the TAP-tag (Rigaut et al. 1999) at the C terminus of Khd1p (Khd1p-TAP) had no growth defect and *ASH1* mRNA was localized at the bud-tip. Furthermore, its target, the HO endonuclease was properly repressed in daughter cells, indicating that the addition of a TAP-tag to Khd1p does not impair function (data not shown). Extracts were prepared from cells grown to midlog phase in rich medium, and RNP complexes were recovered by affinity selection on Immunoglobulin G (IgG)-coated beads and subsequent cleavage with tobacco-etch virus (TEV) protease as described previously (Gerber et al. 2004). About 3 μg of RNA from the Khd1p-TAP affinity-isolated samples was obtained from 1 L cultures. Total RNA isolated from extracts (input) and RNA isolated from affinity-purified Khd1p were used to prepare cDNA probes labeled with different fluorescent dyes, which were then mixed and hybridized to *Saccharomyces cerevisiae* cDNA microarrays. The ratio of the fluorescent hybridization signals from the two differentially labeled RNA samples, at the array element representing each specific gene, provides an assay for enrichment of the corresponding mRNA by the Khd1p-TAP affinity procedure (Gerber et al. 2004).

We have previously shown that *ASH1* mRNA coimmunoprecipitates with Khd1p (Irie et al. 2002), providing an internal positive control for the affinity isolation procedure. Indeed, *ASH1* mRNA was significantly ($P < 0.00075$) enriched in three Khd1p-TAP affinity isolations (average ratio=5.7 ± 1.3) compared with four control isolations with untagged cells (=mock; average ratio=1.56 ± 1.23). To define a list of likely Khd1p RNA targets, we compared association of transcripts from the Khd1p affinity isolations with the mock isolates by two-class significance analysis of microarrays (SAM) and determined false discovery rates (FDRs) for each mRNA (an estimate of the fraction of falsely called associated mRNAs; Tusher et al. 2001). A total of 1279 arrayed sequences, representing 1210 distinct ORFs, were associated with Khd1p-TAP with a FDR of <0.1% (Fig. 1A; for a list of all Khd1p targets, see Supplemental Table S1). This represents ~20% of the known and predicted protein-coding sequences in the *S. cerevisiae* genome. Many of these transcripts code for proteins that share functional related themes, which is reflected by common gene ontology (GO) annotations (Supplemental Table S2). Most striking, a significant fraction of the bound messages encode proteins that are localized to the cell periphery. This includes more than half of the genes assigned to the GO term "cell-wall" (52 out of 98 genes, $P < 10^{-10}$) and one-third (86) of the 258 genes assigned to the GO term "plasma membrane" ($P < 3 \times 10^{-5}$). Khd1p also associated with many mRNAs coding for nuclear proteins preferentially involved in transcriptional regulation ($P < 10^{-4}$) and with diverse factors guiding cellular morphogenesis and structure ($P < 10^{-3}$).

Our list of Khd1p mRNA targets also includes 12 of the 24 known bud-tip-localized mRNAs in yeast (Fig. 1B, *MTL1*, *MID2*, *SRL1*, *WSC2*, *EGT2*, *YPL066w ASH1*,

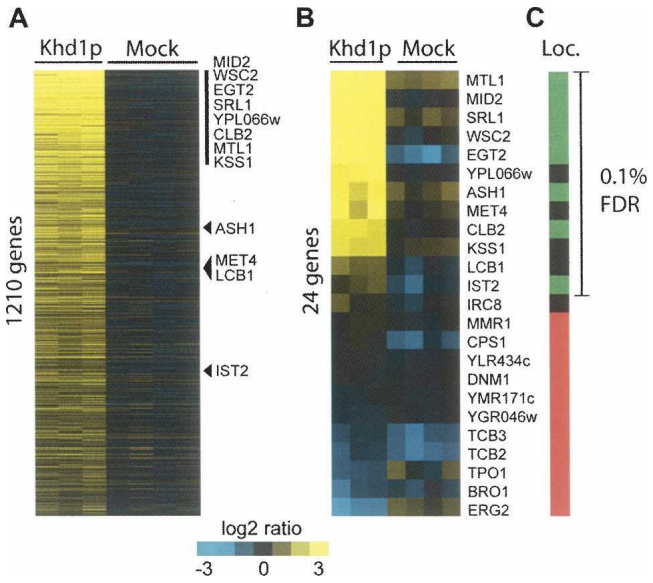

FIGURE 1. Relative enrichment of Khd1p mRNA targets. Three experiments with affinity-tagged Khd1p and four mock experiments are shown. Rows represent genes (unique DNA elements) and columns represent individual experiments. The color code indicates the degree of enrichment (blue, yellow $\log_2$ ratio scale). (*A*) Selected genes were ordered from *top* to *bottom* according to increasing FDRs determined by SAM analysis (FDR <0.1%). Arrowheads depict known bud-tip-localized messages. (*B*) Relative enrichment of 24 bud-tip-localized mRNAs (Shepard et al. 2003). Genes were ordered from *top* to *bottom* according to decreasing average enrichment in Khd1p affinity isolations. (*C*) Colocalization of Khd1p with a subset of mRNAs at the bud-tip of living yeast cells. Assays were done as described in Figure 3. (Green) Colocalization, (red) no-colocalization, (black) not analyzed.

MET4, *CLB2*, *KSS1*, *LCB1*, *IST2*; Takizawa et al. 2000; Shepard et al. 2003). These results were further corroborated by semiquantitative reverse-transcription (RT)–PCR analysis: the mRNAs for *MTL1*, *MID2*, and *ASH1* were clearly detected in RNA samples from Khd1p affinity isolates, but were not detectable in mock isolates, whereas the nontarget mRNA, *BRO1*, was neither detected in both samples (Fig. 2). We have previously shown that Khd1p colocalizes with *ASH1* mRNA to the bud-tip and possibly represses its translation during transport (Irie et al. 2002). Our microarray analysis of Khd1p mRNA targets suggests that this may not apply to all of the 24 known bud-tip-localized mRNAs, but rather to a subset comprised of 12 messages. Additional RNA-binding proteins, such as Puf6p (Gu et al. 2004), may be required for regulation of these bud-tip-localized transcripts.

Khd1p colocalizes with a subset of bud-localized mRNAs

We reasoned that the 12 bud-tip-localized mRNAs associated with Khd1p would colocalize with Khd1p as previously seen with *ASH1* mRNA (Irie et al. 2002). We therefore systematically tested these mRNAs for colocalization with Khd1p using an established system where U1A-tagged mRNA is marked with green fluorescent protein (GFP) (Takizawa and Vale 2000; Irie et al. 2002; Shepard et al. 2003). In this assay, cells harboring genomically integrated myc-tagged versions of Khd1p (Khd1myc) are transformed with two plasmids: The first plasmid (U1Ap-GFP) expresses a variant of GFP fused to U1A, which is an RNA-binding protein that recognizes a specific RNA sequence, the U1A aptamer. The second plasmid (U1Atag-X) harbors a galactose inducible promoter and four copies of the U1A aptamer sequences fused to the coding sequence and 3′-UTR of the transcript under investigation (Shepard et al. 2003). Cells expressing U1Ap-GFP and U1Atag-ASH1 display a single large GFP particle at the distal tips of daughter cells and myc-tagged Khd1p (Khd1myc) colocalizes with this particle in fixed cells (Fig. 3, *ASH1*; Irie et al. 2002). This colocalization merely reflects the in vivo association of Khd1p with tagged mRNA, because no colocalization can be seen in Khd1 mutant cells (Khd1myc-L284N), where the highly conserved Leu-284 residue in the third KH domain is changed to Asn that strongly reduces the binding of Kdh1p to RNA (Fig. 3, bottom; also see Fig. 7C, below). Notably, this finding is consistent with the previous observation that the analogous mutation in the third KH domain of human hnRNP K (I410N) strongly reduces RNA-binding activity (Siomi et al. 1994).

We found that Khd1myc colocalizes with GFP particles derived from *MID2*, *MTL1*, *WSC2*, *EGT2*, *SRL1*, *CLB2*, and *IST2* transcripts, which are all among our experimentally determined mRNA targets by microarray analysis (Figs. 1C, 3). Similar to *ASH1*, Khd1myc-L284N did not colocalize with these GFP particles (data not shown). Khd1myc did not colocalize with the GFP particles derived from *BRO1*, *CPS1*, *DNM1*, *ERG2*, *MMR1*, *TCB2*, *TCB3*, *TPO1*, *YGR046w*, *YLR434c*, and *YMR171c* transcripts (Figs. 1C, 3) confirming our microarray data classifying them as nontargets. We did not test *KSS1*, *LCB1*, *MET4*, and *YPL066w* transcripts for colocalization with Khd1p, because these messages give only few GFP particles, indicating that they are only partially localized in this assay and thus difficult to quantify

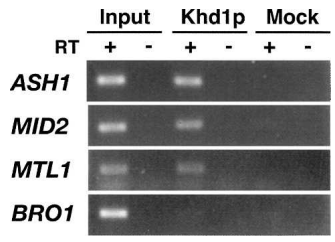

FIGURE 2. Khd1p associates with a subset of bud-tip-localized mRNAs. *ASH1*, *MID2*, and *MTL1* mRNAs, but not *BRO1* mRNA, were detected by RT–PCR in RNAs isolated from total extracts (Input) and from Khd1p-TAP affinity isolations (Khd1p). By comparison, no detectable *ASH1*, *MID2*, *MTL1*, or *BRO1* mRNA was amplified from the Mock control. Control reactions without RT (−) are shown next to samples performed with RT (+). The results shown are representative of two independent experiments.

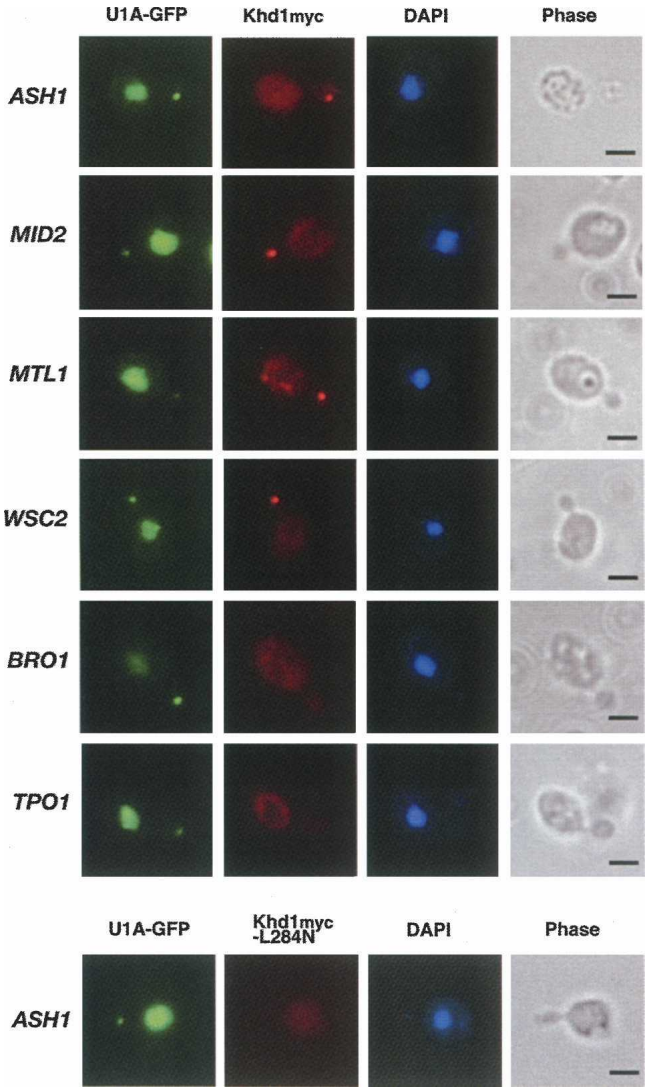

FIGURE 3. Khd1p colocalizes with a subset of mRNAs at the bud-tip of yeast cells. Representative examples for localization of GFP-RNA (green) and myc-tagged Khd1p (red) in fixed yeast cells. Cells stained with 4′,6-Diamidino-2-phenylindol (DAPI) to visualize the nucleus (blue) and phase contrasts images are shown to the *right*. The U1A-GFP-tagged RNAs for *ASH1, MID2, MTL1*, and *WSC2* colocalized with Khd1p, whereas *BRO1* and *TPO1* mRNAs did not colocalize. The U1A-GFP tagged RNA for *ASH1* did not colocalize with Khd1p-L284N. Bar, 2 μm.

(Shepard et al. 2003). In summary, the colocalization data were fully consistent with our microarray analysis of Khd1p targets supporting the reliability of this genome-scale screen to identify Khd1p substrates.

Khd1p associates with the coding regions of the *ASH1, MID2, MTL1,* and *WSC2* mRNAs in vivo

ASH1 mRNA contains three or four *cis*-acting elements that are essential for RNA localization by She protein: N (nucleotides 31–841; numbering starts at the first nucleotide of the start codon), C (nucleotides 1125–1445) and U (nucleotides 1758–1835) (Fig. 4A; Gonzalez et al. 1999) or E1 (nucleotides 598–750), E2A (nucleotides 1044–1196), E2B (nucleotides 1175–1447), and E3 (nucleotides 1750–1868) (Fig. 4A; Chartrand et al. 1999). These elements are located within the coding region (N, C, E1, E2A, and E2B elements) or in 3′-UTRs (U, E3 elements) of *ASH1* mRNA and contain a loop–stem–loop structure that further specifies She2p binding (Jambhekar et al. 2005; Olivier et al. 2005). We have previously shown that Khd1p associates with the N element (Irie et al. 2002), and Paquin et al. (2007) proposed that recombinant Khd1p binds to the E1 element located within the N element in vitro. To further determine the RNA-binding specificity of Khd1p on different substrates, we tested *ASH1*, *MID2*, *MTL1*, and *WSC2* mRNAs for colocalization with Khd1myc in vivo (Fig. 4; Supplemental Table S3). As expected, Khd1p colocalized with transcript of *ASH1*, covering the first 804 nucleotides (nt) of the coding regions that encompasses the E1 element (Fig. 4A; Irie et al. 2002). Khd1p did not colocalize with other regions of ASH1-GFP particles like the E2A and E2B elements (nucleotides 828–1764) located in coding sequences, or the E3 element in the 3′-UTR (Fig. 4A; Supplemental Table S3). We further defined the region required for colocalization with hybrid constructs where fragments of ASH1 coding sequences were fused to the 3′-UTR (1-804 + 3′-UTR, 1–600 + 3′-UTR, 1–486 + 3′-UTR, 1–250 + 3′-UTR, 251–600 + 3′-UTR). This construction was necessary because at least one localization element (E3) is required for localization of the transcripts to the bud-tip by She proteins. Analysis of these constructs revealed that nucleotides 251–600 of the *ASH1* are sufficient for efficient colocalization with Khd1p (Fig. 4A; Supplemental Table S3). However, Khd1p may also weakly associate with other regions in the RNA because *ASH1* mRNA lacking the region 251–600 still partially colocalized with Khd1myc (Fig. 4A) (FullΔ251–600). However, the efficiency of colocalization with this transcript was considerably lower (16 ± 13% of GFP particles) compared with the *ASH1* full-length construct (90 ± 12% of GFP particles) or to nucleotides 251–600 of *ASH1* (67 ± 4.2% of GFP particles), suggesting that this represents a minor or cryptic binding site.

We next mapped the Khd1p-binding regions in *MID2, MTL1*, and *WSC2* transcripts (Fig. 4B–D; Supplemental Table S3). We used hybrid RNAs in which the gene fragments were fused to the 3′-UTR of *ASH1* containing the E3 element, which is necessary for RNA localization to the bud-tip. The addition of *ASH1* 3′-UTR induced the formation of clear GFP particles in the buds and allowed us to easily determine the colocalization of Khd1p to each fragment. These analyses revealed that the *MID2* transcripts bear at least two Khd1p-binding regions in the coding sequence (Fig. 4B; Supplemental Table S3). The first (nucleotides 140–319) colocalized with medium efficiency

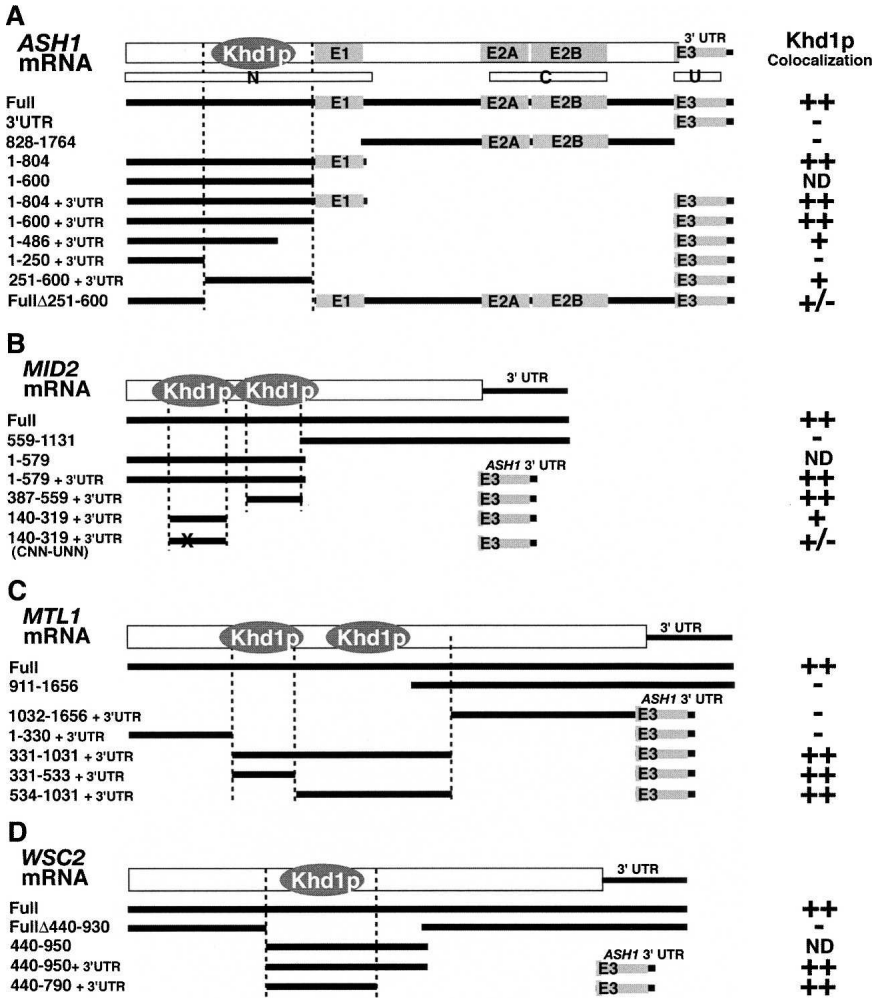

FIGURE 4. Mapping *ASH1, MID2, MTL*, and *WSC2* mRNA regions that are sufficient for colocalization with Khd1p at the bud-tip. (*A*) *ASH1* mRNA, (*B*) *MID2* mRNA, (*C*) *MTL1* mRNA, (*D*) *WSC2* mRNA. Khd1myc tagged cells bearing plasmids expressing U1Ap-GFP (pT220) and U1Atag-X specified to the *left* were examined by immunofluorescence in yeast cells (see Fig. 3). Quantification of Khd1myc colocalization with GFP particles is indicated to the *right*: (++) ≥70% colocalization; (+) 30%–70% colocalization; (+/−) 10%–29% colocalization; (−) <10% colocalization; (ND) not determined. Actual numbers of colocalization are listed as the mean values of at least two independent experiments that were quantified by two independent observers (Supplemental Table S3).

(49 ± 17% of GFP particles), whereas the second regions (nucleotides 389–559) colocalized with very high efficiency (98 ± 2.7% of GFP particles), suggesting strong association of Khd1p with the second region. Similarly, we also identified two regions in the *MTL1* transcript that were sufficient for Khd1p colocalization and encompasses nucleotides 331-533 and 534-1031 in the coding sequence of *MTL1*, respectively (Fig. 4C; Supplemental Table S3). We could also define one Khd1p binding site between nucleotides 440–790 in the coding sequence of *WSC2* (Fig. 4D; Supplemental Table S3). Therefore, in all of our four tested transcripts, Khd1p preferentially associated with coding sequences. This is in contrast to previously characterized KH domain proteins, which bind to sequences located in UTR of mRNAs or to the intron/branchpoint sequences of pre-mRNA (Berglund et al. 1997; Buckanovich and Darnell 1997; Holcik and Liebhaber 1997; Ostareck et al. 1997; Ross et al. 1997; Kanamori et al. 1998). Thus, Khd1p represents a unique member of KH domain proteins.

A repetitive C pattern is present in the coding sequences of Khd1p mRNA targets

We wondered whether there are common structural features within coding sequences of mRNA targets that specify Khd1p binding. Therefore, we retrieved the ORF sequences for the 35 highest scored Khd1p targets and searched for common motifs using multiple expectation maximization for motif elicitation (MEME), a web-based motif search program (see Materials and Methods). This analysis did not reveal a simple short motif that was enriched among the sequences. However, the two top-scored consensus sequences from the MEME analysis beared repetitive patterns of cytosines at every third position in 32 of the 35 searched ORFs (92%), with a median of seven CNN repeats per sequence. No such pattern was found searching 500 bp downstream from or upstream of the ORFs that cover 3′- and 5′-UTR sequences. We next wondered whether similar (CNN) repeats were present among the eight messages for which we have verified colocalization with Khd1p at the bud-tip (Fig. 1B). Indeed, the multiple-sequence alignment of the respective coding sequences revealed the presence of at least six repeats of cytosines at every third position $(CNN)_6$ in all of these transcripts (Fig. 5A). Moreover, the regions containing the minimal $(CNN)_6$ elements matched our experimentally determined regions in mRNAs required for Khd1p colocalization (Figs. 4, 5B). There are extended phases of (CNN) repeats in *MID2* (Figs. 4B, 5B, 387–559), *MTL1* (Figs. 4C, 5B, 331–533), *MTL1* (Figs. 4C, 5B, 534–1031), and *WSC2* (Figs. 4D, 5B, 440–790), and shorter ones are present in three parts of *MID2* (Figs. 4B, 5B, 140–319) and *ASH1* (Figs. 4A, 5B, 251–600) (Fig. 5B). These results let us conclude that the main criteria for Khd1p binding may be phased C's over a certain length (Fig. 5A,B).

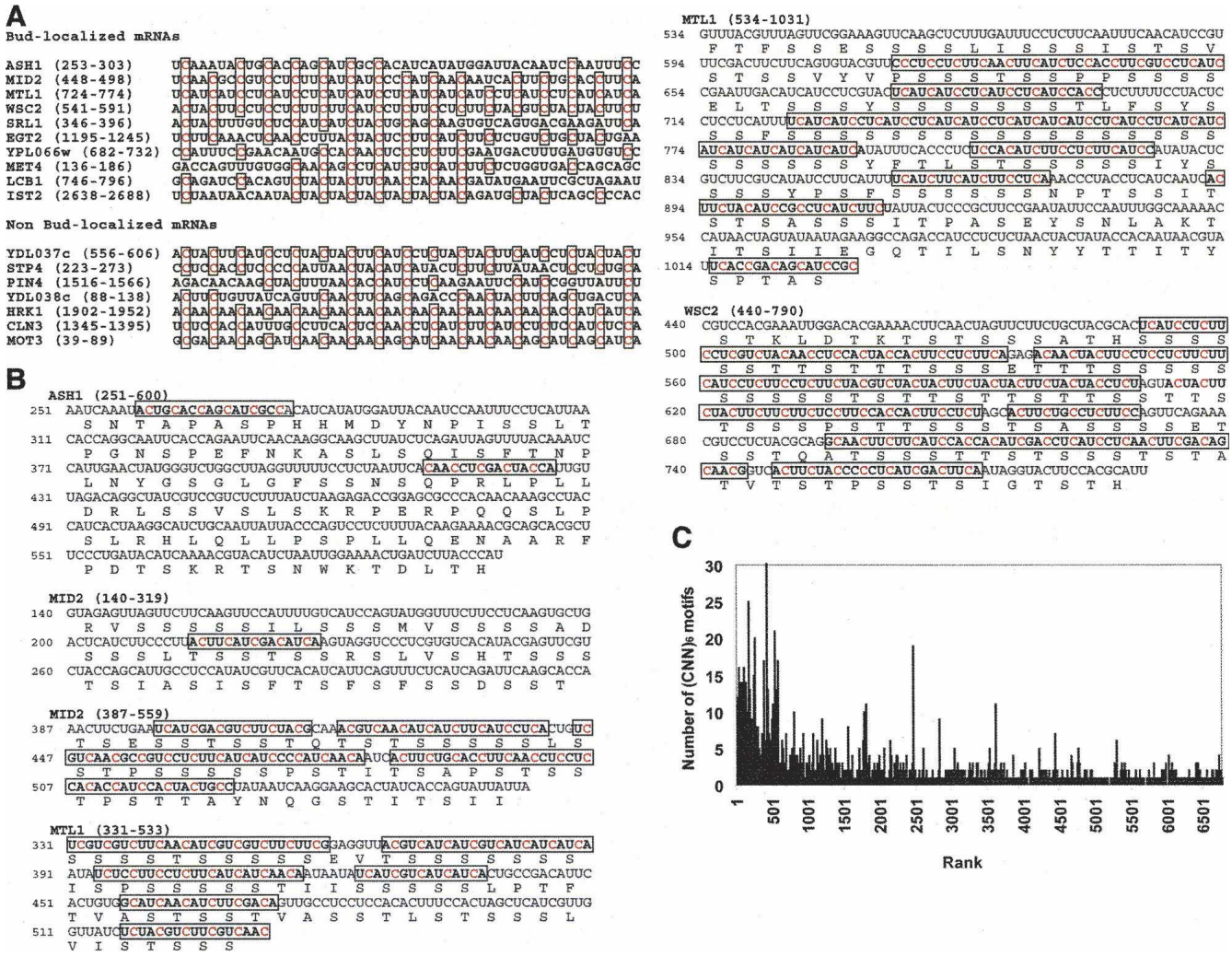

FIGURE 5. Sequence motifs interacting with Khd1p. (*A*) CNN repeats in Khd1p-associated mRNAs. Phased C residues are shown in red and boxed. (*B*) Nucleotide and deduced amino acid sequences of the Khd1p-associated regions of *ASH1*, *MID2*, *MTL1*, and *WSC2* mRNAs. CNN repeats are boxed with C residues highlighted in red. (*C*) Distribution of ORFs with $(CNN)_6$ repeats in Khd1p affinity isolates. Number of (CNN) motifs is plotted on the *y*-axis and ORFs are ranked on the *x*-axis based on decreasing SAM scores for Khd1p association.

If Khd1p binding is guided by CNN repeats, we expect to observe enrichment of this motif among our experimentally defined Khd1p targets (Fig. 5A,B). We therefore searched all yeast ORF sequences for the presence of the minimal element $(CNN)_6$. $(CNN)_6$ occurs 2991 times among 1470 of the 5881 annotated *S. cerevisiae* yeast ORFs (25%). In contrast, 562 of the 1210 (46%) experimentally determined Khd1p targets contain at least one $(CNN)_6$ element in the coding sequence and is therefore significantly over-represented ($P < 10^{-30}$). Moreover, ORFs that bear multiple repeats of the $(CNN)_6$ motif are highly ranked among Khd1p affinity isolates (Fig. 5C; Supplemental Table S1). This could indicate that the number of CNN repeats directly correlates with the binding affinities of Khd1p to the RNA.

The identification of CNN repeats with MEME in the coding sequences among highly scored Khd1p targets mRNAs, the presence of CNN stretches within the experimentally determined regions required for colocalization with Khd1p at the bud-tip, and the significant enrichment of $(CNN)_6$ elements among Khd1p targets strongly suggests that this element represents a major criterion for Khd1p binding in vivo.

Khd1p binds to CNN repeats in *ASH1*, *MID2*, and *MTL1* mRNAs

RNA interactions from affinity purifications and in vivo colocalization assays could also be the result of indirect binding (e.g., through interaction with another RBP). We therefore tested whether Khd1p binds to RNA directly. We produced recombinant glutathione S-transferase (GST)-Khd1p from *Escherichia coli* and monitored binding to in

vitro-transcribed biotinylated-RNAs in RNA pull-down assays. As shown in Figure 6A, GST-Khd1p directly binds to *ASH1*, *MID2*, and *MTL1* mRNAs in vitro, whereas GST did not (data not shown). In contrast, GST-Khd1p did not bind to *TPO1* mRNA, which served as a negative control RNA. We also mapped Khd1p binding to the *MID2* transcripts with RNA pull-down assays (Fig. 6B). Consistent with the colocalization data (Fig. 4B), GST-Khd1p bound to *MID2* fragments comprising nucleotides 140–319 and 387–559 in both assays (Fig. 6B). These results suggest that Khd1p directly binds to its target mRNAs.

We examined Khd1p binding to the *MID2* transcripts with electrophoretic mobility shift assays (EMSA) (Fig. 7). Consistent with the colocalization and RNA pull-down assays (Figs. 4B, 6B), GST-Khd1p bound to *MID2* fragments comprising ntnucleotides 140–319 and 387–559 (Fig. 7A,B). In this assay, the dissociation constant (K_d) of GST-Khd1p and *MID2* RNA (nucleotides 387–559) approximates ~98 ± 22 nM (Fig. 7E), which is in the range of previously measured RNA affinities of KH-domain RBPs (Musunuru and Darnell 2004). Substitution of Leu-284 to Asn in the third KH domain of Khd1p abolished RNA bindings (Fig. 7C), indicating that the third KH domain is mainly required for binding to RNA.

To further examine the binding properties of Khd1p, we performed competition experiments with different sorts of RNA and analyzed binding with EMSA (Fig. 7A,B,D). Consistent with previous observations that Khd1p can bind to poly(C) and poly(U) in vitro (Denisenko and Bomsztyk 2002), poly(C) RNAs competed efficiently and poly(U) RNA competed weakly for Khd1p binding to biotinylated RNA fragments of *MID2* (Fig. 7A,B). The purine bases poly(A) and poly(G) RNAs did not compete for binding at all. Efficient competition with poly(C) supports the idea that Khd1p binds to its target mRNAs though C-rich regions, whereas the slight competition with poly(U) may generally reflect preferences for pyrimidine bases (C/U). The addition of 100-fold excess of $(CNN)_6$ and $(CNN)_{14}$ RNA prevented interaction of biotinylated *MID2* RNA fragments with Khd1, but no such competition was seen with $(NNN)_6$ control RNA (Fig. 7A,B). Thereby, $(CNN)_{14}$ repeats competed more efficiently than $(CNN)_6$ repeats, which supports the previous notion that the length of the repeats positively correlates with binding affinities (Fig. 5C).

To further substantiate the critical role of repetitive cytosines, we substituted all C's to U's in the $(CNN)_5$ of the *MID2* (215–229) (Fig. 5B) and tested the mutant RNA for in vitro binding (Fig. 7D) and in colocalization assays (Fig. 4B). $(CNN)_5$ repeats competed more efficiently than $(UNN)_5$ repeats for Khd1p binding in EMSA (Fig. 7D, CNN_5 versus UNN_5). Likewise, C to U substitution reduced the colocalization of Khd1p with RNA in vivo (Fig. 4B, *MID2*, 140–319 [CNN-UNN]: 14 ± 5.2%; Supplemental Table S3).

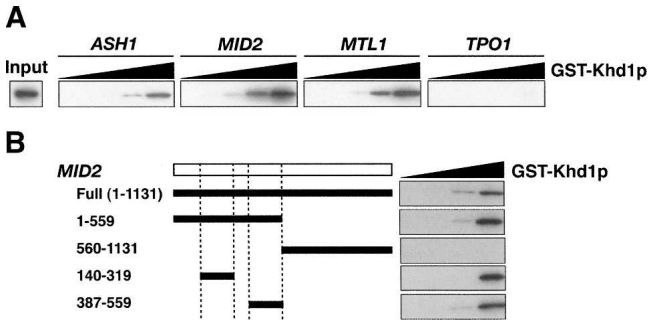

FIGURE 6. Khd1p directly binds to RNAs containing CNN repeats in biotin pull-down assay. (*A*) Pull-down assay with biotinylated RNAs. GST-Khd1p (0.2, 1, 5, and 25 μg) was incubated with in vitro-transcribed and biotinylated RNAs encompassing the *ASH1*, *MID2*, *MTL1*, and *TPO1* coding sequences. RNP complexes were captured with streptavidin beads and GST-Khd1p was detected with anti-GST antibody. GST-Khd1p binds directly to *ASH1*, *MID2*, and *MTL1* mRNAs, but not to *TPO1* mRNA, which is the negative control. (*B*) Biotin pull-down assay. GST-Khd1p (0.2, 1, 5, and 25 μg) was incubated with biotinylated RNAs representing various regions of *MID2*. GST-Khd1p directly binds to the regions 140–319 and 387–559 of *MID2* mRNA.

Khd1p regulates Mtl1p expression at the post-transcriptional level

We have previously shown that *KHD1* overexpression inhibits *ASH1* expression (Irie et al. 2002). Therefore, we systematically examined whether Khd1p modifies protein expression of other bud-tip-localized mRNAs that are bound by Khd1p (*MID2*, *MTL1, WSC2, SRL1, EGT2*, and *CLB2)*. Therefore, we examined strains expressing genomically integrated TAP-tags together with *ADH* 3′-UTR at the C terminus of Ash1, Mid2, Mtl1, Wsc2, and Clb2 ORFs (Egt2p-TAP was not available in our hands) for protein levels by immunoblot analysis. Since Khd1p binds its targets in coding regions, we expect that the TAP-tag at the C terminus should not interfere with the binding of Khd1. In accordance with our previous study, overexpression of Khd1p strongly reduced the levels of Ash1p-TAP to 8.0% (Fig. 8A). Unexpectedly, only Srl1p-TAP was similarly reduced to 21% after induction of Khd1p (Fig. 8A). Most of the tested targets (Mid2p, Wsc2p, Clb2p, and Ist2p) showed no altered protein levels, as did the negative control Bro1p-TAP (nontarget bud-tip-localized gene) (data not shown). Interestingly, Mtl1p protein levels were even increased to 180% after induction of Khd1p, suggesting the Khd1p may have opposing effects on different mRNA targets (Fig. 8B). Notably, we detected a second high molecular weight form of Mtl1p at 250 kD that did not increase upon Khd1p overexpression. This may represent a glycosylated form of Mtl1p, since Mtl1p is predicted to be glycosylated (Rajavel et al. 1999). However, it is currently not known why this high molecular weight form of Mtl1p did not increase upon Khd1p overexpression.

Intrigued by the result that Mtl1 protein levels were increased by Khd1p, we also examined protein levels in *khd1Δ* mutant cells. The *khd1Δ* mutants have reduced levels (11%) of both forms of Mtl1p-TAP compared with wild-type cells (Fig. 8C). Protein levels encoded by other bud-localized mRNAs were not significantly changed in *khd1Δ* mutant cells (data not shown). To exclude the possibility that the addition of TAP-tag and the replacement of endogenous 3′-UTR to *ADH* 3′-UTR affect the regulation by Khd1p, we also examined Mtl1-HA protein level derived from *MTL1-HA-MTL1* 3′-UTR construct. Similar to Mtl1p-TAP, Mtl1p-HA level was decreased in the *khd1Δ* mutants and increased in cells overexpressing *KHD1* (Fig. 8D; data not shown). We also examined *ASH1*-myc, *MID2*-HA, *SRL1*-HA constructs that harbor endogenous 3′-UTR and found that the difference of tag (TAP versus myc/HA) and 3′-UTR (*ADH* or endogenous) did not affect protein levels (data not shown). Thus, in agreement with our previous results on Khd1p binding, it is likely that Khd1p regulates the expression of target mRNAs through the coding sequence rather than the 3′-UTR. Moreover, the reduction of Mtl1p level in the *khd1Δ* mutants could be complemented by wild-type *KHD1* gene, but not *KHD1-L284N* (Fig. 8E), indicating that the regulation of *MTL1* expression by Khd1p is mediated by its RNA-binding activity.

We finally investigated whether Khd1p affects mRNA stability of *MTL1* mRNAs and examined steady-state mRNA levels with Northern blots. The *khd1Δ* mutation reduced the levels of *MTL1* mRNA (Fig. 9A). In contrast, overexpression of *KHD1* increased *MTL1* mRNA levels (Fig. 9B). Similar results were also obtained with the *MTL1-TAP* strain and a probe specific for the *TAP*-tag (Fig. 9C). These results suggest two possibilities for regulation of *MTL1* expression by Khd1p. Khd1p may regulate *MTL1* expression post-transcriptionally through mRNA stability control. Alternatively, Khd1p might regulate *MTL1* expression transcriptionally through the *MTL1* promoter. To examine whether Khd1p regulates *MTL1* expression post-transcriptionally, we measured Mtl1p and *MTL1* mRNA levels derived from a heterologous *GAL* promoter (Figs. 8F, 9D). The Mtl1p and *MTL1* mRNA levels derived from the *GAL* promoter were also decreased in the *khd1Δ* mutants. Similar results were obtained with *ADH* promoter-derived *MTL1* construct (data not shown). These results indicate that Khd1p regulates *MTL1* expression post-transcriptionally via the binding to the coding sequence.

Finally, we measured the decay rates of mRNA by performing transcriptional pulse-chase experiments using the *GAL1p-MTL1* construct. Transcription was first induced in the presence of galactose and then repressed by shifting the medium from galactose to glucose. The mRNA produced by the *GAL1p-MTL1* construct showed a faster decay rate in the *khd1Δ* mutants (Fig. 9E). These results indicate that Khd1p regulates mRNA stability through the binding to CNN repeats in coding sequences. This is an unexpected result, since Khd1p regulates translation of *ASH1* mRNA, but not mRNA stability (Irie et al. 2002; Paquin et al. 2007). Despite the structural similarities for substrate recognition, the regulation of *MTL1* expression is different from that seen for *ASH1* expression, suggesting participation of additional factors that define the fate of each mRNA.

DISCUSSION

Khd1p is required for efficient localization of *ASH1* mRNA to the bud-tip in dividing yeast, possibly acting as a repressor

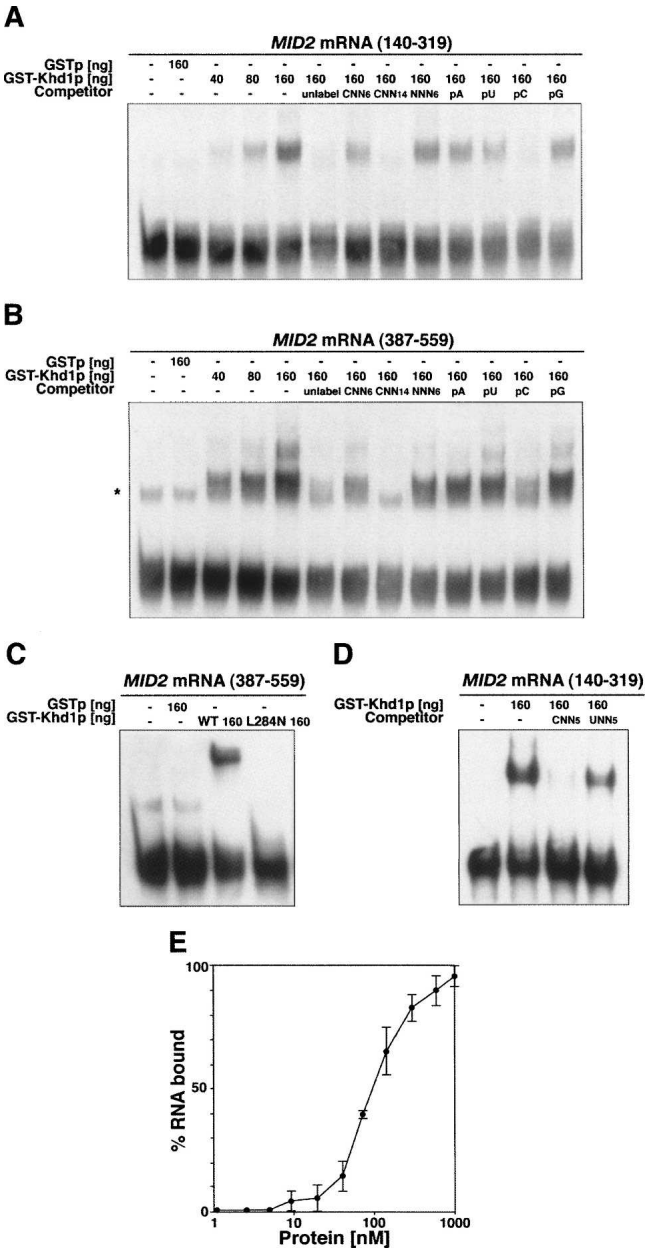

FIGURE 7. (Legend on next page)

of translation during mRNA transport (Irie et al. 2002; Paquin et al. 2007). Khd1p is also involved in the regulation of the telomeric position effect and telomere length (Denisenko and Bomsztyk 2002). Khd1p has been reported to bind poly(C) and poly(U) RNAs in vitro (Denisenko and Bomsztyk 2002) and to interact with 18S and 25S ribosomal and snR10 RNAs in the yeast three-hybrid assay in vivo (Paziewska et al. 2005). However, beside *ASH1*, no other mRNA targets have been known for Khd1p. We have therefore identified target mRNAs for Khd1p on a genome-wide level through the application of a recently established procedure that involves affinity purification of tagged RBPs followed by the analysis of associated RNAs with DNA microarrays (Gerber et al. 2004). We found that Khd1p associates with hundreds of mRNAs comprising almost 20% of the yeast's transcriptome (Fig. 1A). Notably, our experimentally determined Kd value of Khd1p for RNA binding (90 nM) is about 10 times lower than an estimate of Khd1 protein concentration in the cytoplasm (900 nM based on 15,600 copies per cell) (Ghaemmaghami et al. 2003), and thus, it is well possible that most of the mRNA targets are bound to protein (~2000 copies of 1200 target mRNAs [0.1% FDR] calculated based on the data of Holstege et al. [1998] and Wang et al. [2002]). The number of these potential targets for Khd1p regulation appears high compared with the few RNA substrates that were studied for this and other KH-domain RNA-binding proteins and suggest widespread roles of Khd1p in diverse physiological processes. Such extensive binding to hundreds of mRNA targets has been noticed for several other specific RBPs and possibly suggests strong coordinative roles for these proteins in the organization of mRNA "pools" in cells (Gerber et al. 2004; Hieronymus et al. 2004; Halbeisen et al. 2008). Moreover, a significant fraction of the potential Khd1p mRNA targets encode proteins localized to the cell periphery, such as the cell wall and plasma membrane, and nuclear proteins involved in transcriptional regulation (Supplemental Table S2). The functional or cytotopic relation among RNAs targeted by RNA-binding proteins has also been previously observed and provides further evidence for the presence of a highly organized post-transcriptional regulatory system built on functionally related RNA regulons/modules (Gerber et al. 2004, 2006; Hieronymus et al. 2004; Keene 2007; Halbeisen et al. 2008).

Our genomic screen revealed 12 of the 24 known bud-tip-localized mRNAs as potential Khd1p targets (Fig. 1B, *MTL1*, *MID2*, *SRL1*, *WSC2*, *EGT2*, *YPL066w*, *ASH1*, *MET4*, *CLB2*, *KSS1*, *LCB1*, *IST2*) (for a list of all known bud-localized mRNAs, see Takizawa et al. 2000; Shepard et al. 2003). The association of these potential targets was fully confirmed in a secondary screen that visualized colocalization of Khd1p with mRNAs at the bud tip in yeast and, therefore, strongly supports the reliability of our experimental system for the identification of Khd1p targets (Fig. 3). Since Khd1p appears to be involved in temporal and spatial regulation of *ASH1* mRNA translation (Irie et al. 2002; Paquin et al. 2007), this RNA subset may be subject to Khd1p regulation, whereas other bud-tip-localized mRNAs that are not bound by Khd1p may be regulated by distinct RNA-binding proteins such as Puf6p (Gu et al. 2004). Notably, it has been reported that *ASH1* mRNA localization is coordinated at the cortical endoplasmatic reticulum (cortical ER) (Schmid et al. 2006), and that the mRNA is enriched in ER-bound polysomes for translation (Diehn et al. 2000). This correlates well with our observation that Khd1p preferentially associates with mRNAs encoding cell wall and membrane proteins that are translated on ER-bound polysomes, and thus, we speculate that Khd1p may guide mRNAs to ER-bound polysomes.

The combination of bioinformatics and RNA localization studies revealed that Khd1p preferentially associates with CNN repeats in the coding regions of target mRNAs (Figs. 4–7). Khd1p contains three KH-type RNA-binding domains like hnRNP K and PCBPs from human (Denisenko and Bomsztyk 2002; Makeyev and Liebhaber 2002; Bomsztyk et al. 2004). hnRNP K and PCBPs both have poly(C)-binding specificity, and hnRNP K was shown to interact with CU-rich repetitive sequence elements in the 3′-UTR of *15-lipoxygenase* mRNA (Ostareck et al. 1997). The consensus sequence for hnRNP K, $(\underline{C}CC\underline{C}AC\underline{C}CU\underline{C}UU\underline{C}CC\underline{C}AAG)_n$, matches our experimentally determined $(CNN)_n$ element that directs Khd1p binding. However, Khd1p binds within coding sequences, whereas all the previously characterized KH domain proteins, such as ZBP-1, Nova-1, PCBP1/

FIGURE 7. Khd1p directly binds to RNAs containing CNN repeats in electrophoretic mobility shift assays. (*A*,*B*) Electrophoretic mobility shift assay with biotinylated RNAs coding for nucleotides 140–319 (*A*) and nucleotides 387–559 (*B*) of *MID2*. A total of 5 ng (87 fmol) of RNA was incubated with GST (160 ng; negative control) or GST-Khd1p (40, 80, and 160 ng) in binding buffer containing yeast tRNA and heparin as nonspecific competitors. The indicated specific competitors were used to examine the binding specificity of unlabeled nonbiotinylated RNAs, $(CNN)_6$: A$\underline{C}$UU$\underline{C}$UG$\underline{C}$AC$\underline{C}$UU$\underline{C}$AA$\underline{C}$C, $(CNN)_{14}$, A$\underline{C}$UU$\underline{C}$UG$\underline{C}$AC$\underline{C}$UU$\underline{C}$AA$\underline{C}$CU$\underline{C}$CU$\underline{C}$CA$\underline{C}$AC$\underline{C}$AU$\underline{C}$CAC UA$\underline{C}$UG$\underline{C}$C, $(NNN)_6$, $\underline{C}$AAGGAAG$\underline{C}$A$\underline{C}$UAU$\underline{C}$A$\underline{C}$C, pA: poly(A) RNA, pU: poly(U) RNA, pC: poly(C) RNA, pG: poly(G) RNA. (*) Nonspecific band. The reaction mixture was resolved on 5% PAGE and RNA was detected after blotting to a nylon membrane with streptavidin-HRP. The results shown are representative of three independent experiments. (*C*) Khd1p-L284N does not bind to biotinylated RNA coding for nucleotides 387–559 of *MID2*. The experiment was performed as described above with 160 ng of GST-Khd1p-L284N. The results shown are representative of three independent experiments. (*D*) C to U substitution of CNN5 repeats in MID2 (140–319) reduces the affinity to Khd1p. The following specific competitors were used to examine the binding specificity: $(CNN)_5$, GACUCAUCUUCCCUUA$\underline{C}$UU$\underline{C}$AU$\underline{C}$GA$\underline{C}$AU$\underline{C}$AAGUAGGUCCCU C; $(UNN)_5$, GACUCAUCUUCCCUUA$\underline{U}$UU$\underline{U}$AU$\underline{U}$GA$\underline{U}$AU$\underline{U}$AAG UAGGUCCCUC. The results shown are representative of three independent experiments. (*E*) Binding curve measuring Khd1p interaction with biotinylated RNA coding for nucleotides 387–559 of *MID2*. Kd value was calculated from the mean values of three independent experiments with standard deviation.

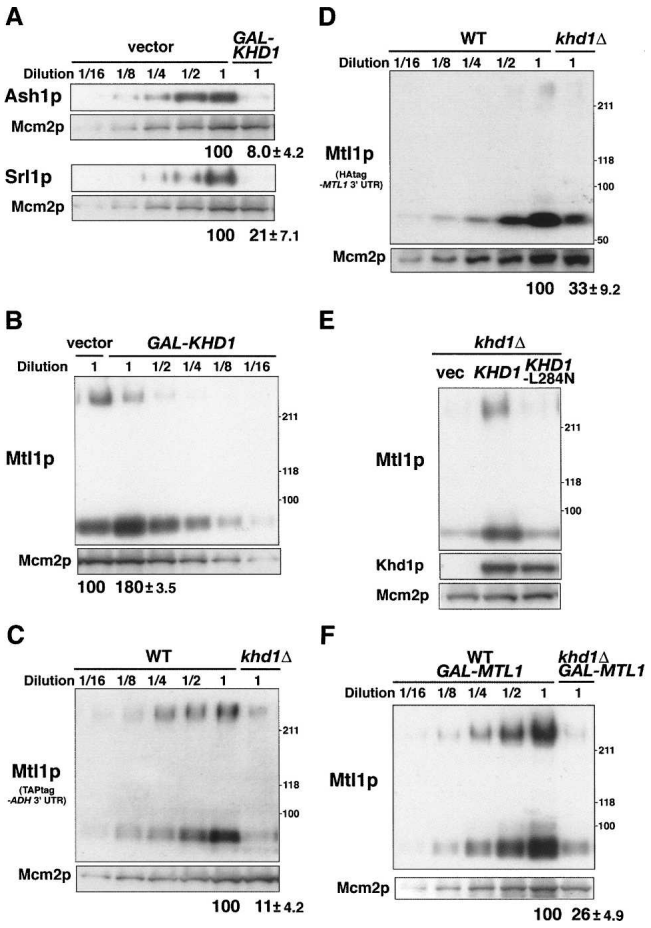

FIGURE 8. Khd1p positively and negatively affects protein levels of its target mRNAs. Protein levels were quantified by Western blotting as described in the Materials and Methods. Mcm2p was included as a quantity control. The level of the tagged proteins are shown as the mean values of three independent experiments with standard deviation. (*A*,*B*) Effect of *KHD1* overexpression on Ash1-TAP, Srl1-TAP (*A*), and Mtl1-TAP (*B*). (*C*,*D*) Effect of *KHD1* deletion (*khd1Δ*) on Mtl1-TAP (*C*), Mtl1-HA (*D*) protein levels. (*E*) KHD1myc, but not KHD1myc-L284N, complements for the decreased level of Mtl1-TAP in *khd1* mutants. (*F*) Effect of *KHD1* deletion (*khd1Δ*) on Mtl1-TAP derived from *GAL1* promoter. Predicted molecular masses: Ash1p, 86 kDa (66 kDa + 20 kDa [TAP-tag]); Srl1p, 83 kDa (63 kDa + 20 kDa [TAP-tag]); Mtl1p: 74 kDa (54 kDa + 20 kDa [TAP-tag]).

hnRNP E, hnRNP K, splicing factor/branch point binding protein, and vigilin, are reported to bind sequences in the 3′-UTR of mRNAs, or to introns and branchpoint sequences in pre-mRNAs (Berglund et al. 1997; Buckanovich and Darnell 1997; Holcik and Liebhaber 1997; Ostareck et al. 1997; Ross et al. 1997; Kanamori et al. 1998). Khd1p is therefore an unusual member of this RBP family that binds to coding sequences and thereby may interfere with translation initiation or elongation.

We noticed that the cytosines at 3rd positions of the Khd1p recognition motif go along with the genetic code (Fig. 5B): the C's are preferentially found at the second position of codons among Khd1p targets (92.5% of the

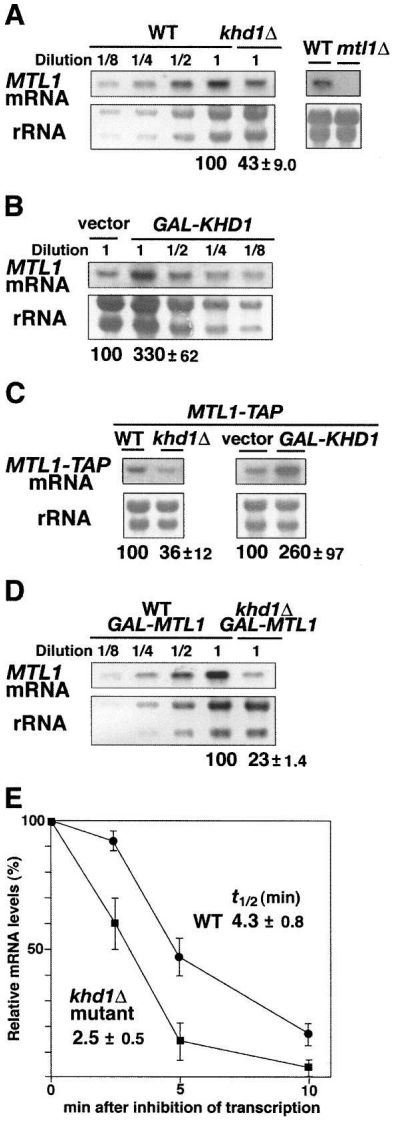

FIGURE 9. Khd1p positively affects mRNA levels of *MTL1*. *MTL1* transcripts were quantified by Northern blotting as described in the Materials and Methods. *MTL1* mRNA probe was used in *A*, *B*, *D*, and *E*. *TAP*tag probe was used in *C*. rRNA was included as a quantity control. The mRNA level is indicated as percentage of wild-type levels and represents the mean of three independent experiments with standard deviation. (*A*) Steady-state *MTL1* mRNA levels in wild-type (WT: 10B), *khd1Δ* cells (YKEN221), and *mtl1Δ* cells. (*B*) *MTL1* mRNA level upon Khd1p overexpression. Empty vector control is indicated to the *left*. (*C*) *MTL1-TAP* mRNA levels in wild-type (WT: MTL1-TAP), *khd1Δ* (MTL1-TAP k), wild-type cell harboring the empty vector (control), and wild-type cell harboring the GAL-KHD1 plasmid. (*D*) *MTL1* mRNA expression under the control of the *GAL1* promoter in wild-type (WT: 10B) and *khd1Δ* mutant cells (YKEN201). (*E*) The half-lives ($t_{1/2}$ min) of *MTL1* transcript in *khd1Δ* mutant. WT: 10B [*pGAL-MTL1-TAP*], *khd1Δ*: YKEN201 [*pGAL-MTL1-TAP*]. The half-lives ($t_{1/2}$ min) were quantified by Northern blotting as described in Materials and Methods.

coding sequences bearing the minimal $[CNN]_6$ repeat element), which translates into stretches of the four amino acids proline (Pro), serine (Ser), threonine (Thr), or alanine (Ala). *MID2*, *MTL1*, and *WSC2* encode Ser-rich membrane proteins—an amino acid often found among cell wall proteins that are glycosylated. Whether preferential binding of Khd1p to mRNAs encoding membrane and cell wall proteins provides a means to link translation to glycosylation has to be further investigated.

The impact on Khd1p on gene expression was monitored in cells overexpressing of *KHD1* and in *khd1Δ* mutants (Fig. 8). *KHD1* overexpression resulted in reduced cellular levels of the Ash1 and Srl1 proteins, but on the other hand, led to increased levels of Mtl1 protein. No changes were observed for four other bud-tip-localized Khd1p targets. In the reverse experiment, namely, testing of protein levels in *khd1Δ* mutants, Mtl1p was the only protein with altered steady-state levels (Fig. 8). Moreover, we found that *KHD1* overexpression or *khd1Δ* mutation differentially affected the amount *MTL1* mRNA likely by regulating its stability, which was unexpected because this result is opposite to the known role of Khd1p as a translational regulator of *ASH1* where mRNA levels are not affected (Irie et al. 2002). Thus, Khd1p positively and negatively influences expression of target genes in at least two different ways: it mediates translational control as seen for *ASH1* and *SRL1* mRNAs, and it affects mRNA stability as exemplified for *MTL1* mRNA. Since translationally arrested mRNAs are targeted to processing bodies and can be eventually degraded (Parker and Sheth 2007), the enhanced decay of *MTL1* mRNA in the *khd1Δ* mutant cells might be the result of decreased translation. Similarly, it has been reported that Puf proteins can also control both translation and mRNA stability, although the regulation is mediated by the binding to sequence elements in 3′-UTRs (Wickens et al. 2002).

How then does Khd1p differentially regulate the expression of target mRNAs? Paquin et al. (2007) recently demonstrated that Khd1p interacts with the C-terminal domain of eIF4G1, inhibiting translation through direct interaction with the coding sequences of *ASH1* mRNA. Our results indicate that this type of regulation may not apply to all of the targets. Instead, we postulate that Khd1p has different partners that determine individual mRNA fates. Khd1p together with eIF4G represses the translation of some target mRNAs such as *ASH1* and *SRL1* mRNAs. On the other hand, Khd1p may collaborate with another protein to stabilize other target mRNAs like *MTL1*. It should be noted that neither *KHD1* overexpression nor *khd1Δ* mutation affects the expression of *MID2*, *WSC2*, and other mRNAs, although Khd1p associates and colocalizes to these mRNAs in vivo. In these cases, Khd1p might regulate the translation and/or mRNA stability under specific circumstances. Alternatively, on these mRNAs, translational inhibition and mRNA stabilization by Khd1p might be just balanced. It will be of future interest to investigate how the plethora of Khd1p mRNA targets are coordinately regulated by Khd1p and what are the physiological implications of this regulation. Despite the many mRNA targets, the *khd1Δ* mutant has no drastic phenotype in rich media except for the partial delocalization of *ASH1* mRNA and protein resulting in slightly reduced expression of *HO* and the reduced expression of Mtl1p. However, it has been reported that *khd1Δ* mutants are highly sensitive to two related antifungal glycopeptides, Stichloroside and Theopalauamide (Parsons et al. 2006). Thus, Khd1p-mediated regulation of target mRNAs may be only required for the cell growth under specific circumstances. Alternatively, the lack of drastic phenotypes may indicate that Khd1p—and possibly many other RNA-binding proteins—are actors in a highly redundant and thus more robust post-transcriptional regulatory system.

MATERIALS AND METHODS

Strains and general methods

Strains used in this study are described in Supplemental Table S3. TAP-tagged Khd1p, Ash1p, Mid2p, Mtl1p, Wsc2p, Clb2p, Srl1p, Ist2p, and Bro1p strains (BY4741 back ground; *MATa his3Δ1 leu2Δ0 met15Δ0 ura3Δ0*) were obtained from Open Biosystems (Ghaemmaghami et al. 2003). The myc-tagged Khd1p strain (YKEN203) was used to monitor colocalization with RNA particles (Irie et al. 2002). The HA-tagged Mtl1p strain was constructed by the method of Longtine et al. (1998) with a PCR fragment generated from plasmid pFA6a-3HA-MTL1 3′-UTR-kanMX6. Standard procedures were followed for yeast manipulations (Kaiser et al. 1994). The media used in this study included rich medium, synthetic complete medium (SC), and synthetic minimal medium (SD) (Kaiser et al. 1994). SC media lacking amino acids or other nutrients (e.g., SC-Ura corresponds to SC lacking uracil) were used to select transformants. SR and SG were identical to SC except that it contained raffinose and galactose, respectively, instead of 2% glucose. Recombinant DNA procedures were carried out as described (Sambrook et al. 1989).

Affinity isolation of Khd1p and identification of bound RNAs with DNA microarrays

TAP-tagged Khd1p was purified from 1 L of cells grown in yeast-peptone-dextrose (YPD) medium as previously described (Gerber et al. 2004). cDNA was synthesized from 3 μg of total RNA derived from the extract and 500 ng of affinity-isolated RNA and labeled with Cy3 and Cy5 fluorescent dyes, respectively. The samples were mixed and hybridized on cDNA microarrays containing features representing all *S. cerevisiae* ORFs, introns, and the mitochondrial genome (Gerber et al. 2004). Arrays were scanned with an Axon Instruments Scanner 4000, data were collected using GENEPIX 3.1 (Molecular Devices) and normalized computationally by the Stanford Microarray Database (SMD) (Demeter et al. 2007). Log_2 median ratios from three independent Khd1p affinity isolations and four mock control isolations (Gerber et al. 2004) were retrieved from SMD and filtered for regression correlation of >0.6 and for signal over background >1.8

in the channel measuring total RNA from extract. Only features that met this criterion in >60% of the arrays were further considered (6761 features) and data were exported into Microsoft Excel. To identify transcripts that were specifically enriched with Khd1p, two-class Significance Analysis of Microarrays (SAM, version 3.02) (Tusher et al. 2001) was performed using *t*-test statistics on median centered arrays. We selected the RNA targets by the following criteria: FDR <0.1%, average enrichment in Khd1p affinity isolations greater than zero, and data were present in at least two of three independent Khd1p affinity isolations. This analysis resulted in 1279 features representing 1210 ORF genes (19% of all analyzed features) (Supplemental Table S1). Microarray data sets are available at the SMD or at the Gene Expression Omnibus at http://www.ncbi.nlm.nih.gov/geo (GEO accession numbers GSE10279 and GSM259462–GSM259468).

RT-PCR analyses with RNAs isolated from extracts and from Khd1p-TAP affinity isolations were performed as previously described (Irie et al. 2002). The number of amplification cycles was adjusted to avoid reaching a plateau phase during PCR. Primer sets are listed in Supplemental Table S6.

Bioinformatics

Significantly shared GO annotations for our defined Khd1p RNA targets were searched with the GO Term Finder found at the *Saccharomyces* Genome Database (SGD; http://db.yeastgenome.org/cgi-bin/GO/goTermFinder.pl) considering background gene set with all features that passed array filtering (total 6109 genes with GO annotations). For motif searches with nucleotide sequences, the sense strand was searched with the MEME program under the proposed default settings at http://meme.sdsc.edu/meme/website/meme.html (Bailey and Elkan 1994).

Plasmids

Plasmids used in this study are described in Supplemental Table S4. Plasmid pPT120 expresses U1Atag-ASH1 from the *GAL1* promoter (Takizawa and Vale 2000). Plasmid pPT220 expresses U1A-GFP-GST-NLS from the *TDH3* promoter (Takizawa and Vale 2000). Plasmids U1Atag-MID2, U1Atag-MTL1, U1Atag-WSC2, U1Atag-EGT2, U1Atag-SRL1, U1Atag-CLB2, U1Atag-IST2, U1Atag-BRO1, U1Atag-CPS1, U1Atag-DNM1, U1A-ERG2, U1Atag-MMR1, U1Atag-TCB2, U1Atag-TCB3, U1Atag-TPO1, U1Atag-YGR046w, U1Atag-YLR434c, U1Atag-YMR171c, U1Atag-KSS1, U1Atag-LCB1, U1Atag-MET4, and U1Atag-YPL066w were a gift from Drs. Kelly Shepard and Ron Vale (University of California at San Francisco) (Shepard et al. 2003). Plasmid pK736 is YEpURA3 plasmid carrying *GAL1p-KHD1* (Irie et al. 2002). Plasmid pCgLEU2 is pUC19 carrying the *C. glabrata LEU2* gene (Sakumoto et al. 1999). pFA6a-3HA-MTL1 3′-UTR-kanMX6 was constructed by a replacement of *ADH 3′-UTR* in pFA6a-3HA-kanMX6 (Longtine et al. 1998) with *MTL1 3′-UTR*, which was cloned with the primer set of i646 and i647 (Supplemental Table S6). Plasmid Khd1myc-L284N, where the highly conserved Leu-284 residue in the third KH domain is changed to Asn, was constructed by PCR with the primer set of i625 and i626.

The following plasmids were constructed to map Khd1p-associated regions in the *ASH1*, *MID2*, *MTL1*, and *WSC2* mRNAs with RNA localization assays (nucleotide postions in ORFs are indicated in brackets): U1Atag-ASH1 3′-UTR, U1Atag-ASH1 (828–1764), U1Atag-ASH1 (1–804), U1Atag-ASH1 (1–600), U1Atag-ASH1 (1–804 + 3′-UTR), U1Atag-ASH1 (1–600 + 3′-UTR), U1Atag-ASH1 (1–486 + 3′-UTR), U1Atag-ASH1 (1–250 + 3′-UTR), U1Atag-ASH1 (251–600 + 3′-UTR), U1Atag-ASH1 (FullΔ251–600), U1Atag-MID2 (559–1131), U1Atag-MID2 (1–579), U1Atag-MID2 (1–579 + 3′-UTR), U1Atag-MID2 (140–329 + 3′-UTR), U1Atag-MID2 (387–559 + 3′-UTR), U1Atag-MID2 (140–329[CNN-UNN]+3′-UTR), U1Atag-MTL1 (911–1656), U1Atag-MTL1 (1–330 + 3′-UTR), U1Atag-MTL1 (331–1031 + 3′-UTR), U1Atag-MTL1 (331–533 + 3′-UTR), U1Atag-MTL1 (534–1031 + 3′-UTR), U1Atag-WSC2 (FullΔ440–930), U1Atag-WSC2 (440–950), U1Atag-WSC2 (440–950 + 3′-UTR), and U1Atag-WSC2 (440–790 + 3′-UTR). The sequence of each region was amplified by PCR from plasmid DNA with appropriate primers (Supplemental Table S6) and subcloned into pGEM-T vector (Promega). The PCR products, the fragment containing *GAL1p*-U1Atag, and the fragment containing *ASH1* 3′-UTR were inserted into pRS426 (Sikorski and Hieter 1989).

Gene deletion

Deletion of *KHD1* was performed by the PCR-based gene-deletion method (Baudin et al. 1993; Schneider et al. 1996; Sakumoto et al. 1999; Tadauchi et al. 2001). Primer sets OKEN163 and OKEN164 (Supplemental Table S5) were designed such that 46 bases at the 5′ end of the primers were complementary to those at the corresponding region of the target gene, and 20 bases at their 3′ end were complementary to the pUC19 sequence outside of the polylinker region in the plasmid pCgLEU2 containing the *Candida glabrata LEU2* gene as a selectable marker. Primer sets for PCR were designed to delete the ORF completely. The PCR products were transformed into the wild-type strain and selected for Leu^+. All gene disruptions were verified by colony-PCR (Huxley et al. 1990).

Induction and imaging of U1Atagged RNA particles

Colocalization of myc-tagged proteins with U1Atagged RNA particles was examined as described previously (Takizawa and Vale 2000; Irie et al. 2002). Cells containing U1Ap-GFP and U1Atag-X were grown overnight at 30°C in SR-UraTrp or SR-HisTrp medium. Overnight cultures were adjusted to an optical density (OD) of 0.5 (600 nm) in SR-UraTrp or SR-HisTrp medium and further grown for 2 h at 30°C. Galactose was added to 0.2%, and the cultures incubated for 2 h at 30°C. Cells were examined by phase contrast microscopy using a X100 magnification and NA 1.4 lens (Carl Zeiss). Images were captured with a cooled charged-coupled device (Carl Zeiss) and digital images displayed with Adobe Photoshop (Adobe Systems, Inc.). For colocalization experiments, samples were fixed with 3.7% formaldehyde for 1 h. Cells were washed with PBS and made into spheroplasts in SP buffer (100 mM phosphate buffer at pH 7.0, 1.2 M sorbitol containing 30 mM mercaptoethanol, 40 mg/mL zymolyase 100T) for 30 min at 37°C. Spheroblasts were washed once with SP buffer and spread onto polylysine-coated, multiwell slides, and incubated with monoclonal anti-myc antibody 9E10 (Santa Cruz Biotechnologies Inc.) at 1:1,000 dilution in blocking buffer (PBS, 1% BSA) for 1 h. After washing, cells were incubated with rhodamine-conjugated goat anti-mouse IgG (Boehringer Mannheim) in blocking buffer for 1 h. Cells were washed and mounted in mounting buffer (Fluoromount-G [Southern Biotech]

containing 0.1 μg/mL 4′,6-diamidino-2-phenylindole). To quantify colocalization of Khd1p with GFP particles, >50 premitotic cells with small to medium buds were identified and scored for the signals for Khd1p versus the GFP particles. Colocalization was defined as clear merged yellow signal resulting from a merge of red (Khd1myc) and green (GFP) channel with the AxioVision LE program (Carl Zeiss). Colocalization was quantified as described (full data listed in Supplemental Table S2; Shepard et al. 2003). Colocalization was analyzed in at least two independent experiments by two independent observers.

RNA pull-down assay

A GST fusion vector containing *KHD1* was constructed with pGEX5X-1 (Amersham Biosciences). Therefore, the EcoRI–SalI fragment of the *KHD1* coding sequence was amplified by PCR with primers i305 and i306 (Supplemental Table S5) and inserted into the EcoRI–SalI sites of pGEX5X-1. The GST-Khd1 fusion protein was purified with glutathione-sepharose beads as indicated by the manufacturer (Amersham Biosciences). Biotinylated mRNAs were produced by in vitro run-off transcription with the MEGAscript T7 transcription kit (Ambion) and biotin-11-CTP. GST-Khd1p proteins (0.2, 1, 5, and 25 μg) were incubated with 5 μg of biotinylated mRNAs in 500 μL of binding buffer (10 mM Hepes-KOH at pH 7.5, 5% Glycerol, 5 mM $MgCl_2$, 40 mM KCl, 1 mM dithiothreitol, 1.5 μg/μL BSA, 67 ng/μL yeast tRNA, 1.5 μg/μL heparin, 0.2 U/μL RNasin). Yeast tRNA and heparin were added as nonspecific competitors. mRNA–protein complexes were isolated with streptavidin beads, washed three times, and the samples were subjected to Western blot analysis to detect GST-Khd1p with anti-GST antibody (Santa Cruz Biotechnologies Inc.: 1:1000).

Electrophoretic mobility shift assay

A total of 5 ng (87 fmol) of biotinylated RNA encompassing nucleotidess 140–319 or 387–559 of the *MID2* ORFs were incubated with GST (160 ng) or GST-Khd1p (40, 80, 160 ng) in 20 μL of the binding buffer (10 mM Hepes-KOH at pH 7.5, 2.5% glycerol, 5 mM $MgCl_2$, 40 mM KCl, 1 mM dithiothreitol, 67 ng/μL yeast tRNA, 1.5 μg/μL heparin, 0.2 U/μL RNasin). Yeast tRNA and heparin were added as nonspecific competitors. The following RNAs were used for specific competition experiments:

$(CNN)_6$, ACUUCUGCACCUUCAACC;
$(CNN)_{14}$, ACUUCUGCACCUUCAACCUCCUCCACACCAUCCACUACUGCC;
$(NNN)_6$, CAAGGAAGCACUAUCACC;
$(CNN)_5$, GACUCAUCUUCCCUUACUUCAUCGACAUCAAGUAGGUCCCUC;
$(UNN)_5$, GACUCAUCUUCCCUUAUUUUAUUGAUAUUAAGUAGGUCCCUC; and
poly (A) RNA, poly (U) RNA, poly (G) RNA, poly (C) RNA (Sigma).

The reaction mixture was resolved on a native 5% polyacrylamide gel, followed by electroblotting onto positively charged nylon membrane (Roche). Blots were blocked for 30 min at room temperature in 1% blocking reagent (Roche) in maleic acid buffer (0.1 M maleic acid, 0.15 M NaCl at pH 7.5). Blots were probed with streptavidin-HRP (GE Healthcare: 1:1000), washed three times with TBS buffer, and developed with enhanced chemiluminescence detection kit (Amersham).

Preparation of yeast extracts and Western blot analysis

Five milliliters of yeast cells were grown to OD_{600} = 0.5–1 in SR-ura medium and Khd1p expression was induced for 2 h by the addition of 2% galactose. Cultures were quickly chilled on ice and collected by centrifugation. The pellet was washed twice with PBS and resuspended in 100 μL of breaking buffer (4% SDS, 40 mM Tris-HCl at pH 7.0, 8 M urea, 0.1 mM EDTA, 1% 2-mercaptoethanol). Glass beads (0.4–0.6 mm diameter) were added and cells were broken by vigorous vortexing for 5 min at room temperature. Beads and cell debris were removed by centrifugation at 14,000 rpm at room temperature. Protein concentrations of the cell extracts were measured at OD 280 nm. Extracts were subjected to SDS-PAGE on 8% acrylamide gels, followed by electroblotting onto an Immobilonmembrane (MILLIPORE). To detect the TAP-tagged proteins, the blots were blocked for 30 min at room temperature with TBS-M buffer (20 mM Tris-HCl at pH 7.5, 150 mM NaCl, 5% nonfat dry milk) and further incubated with peroxidase-anti-peroxidase soluble complex (PAP; Sigma) diluted 1:4000 in TBS-M buffer overnight at 4°C. After three final washes with TBS buffer, blots were developed with the enhanced chemiluminescence detection kit (Amersham). To control for equal loading of the lanes, the blots were probed with anti-Mcm2 antibody (Santa Cruz Biotechnology Inc.: 1:1000) and peroxidase-conjugated secondary antibody (Calbiochem: 1:3000).

Nothern blot analysis

Total RNAs were prepared from cells with ISOGEN reagent (Nippongene). RNA samples were loaded on a 1% agarose gel containing 5.5% formaldehyde and resolved by electrophoresis. RNA was transferred to a nylon membrane and then hybridized with digoxigenin-labeled antisense probe. The primers sets, i499 and i502, and TN264 and TN266 (Supplemental Table S6) were used to detect *MTL1* mRNA and *MTL1-TAP* mRNA, respectively. After washing and blocking, the membrane was incubated with alkaline phosphatase-conjugated anti-DIG antibody, and the signal was detected by enhanced chemiluminescence.

The half-lives ($t_{1/2}$ min) were determined from Northern blots as described previously (Tadauchi et al. 2001; Inada and Aiba 2005). Cells were grown in SG-Ura, and the medium was changed to SC-Ura to inhibit transcription from *GAL1* promoter. Cells were harvested at the indicated times and total RNA was isolated. Samples were analyzed by Northern blots with specific probes, and half-lives ($t_{1/2}$ min) were determined as the mean from three independent experiments. rRNA was used as a reference for quantification.

SUPPLEMENTAL DATA

Supplemental material can be found at http://www.rnajournal.org.

ACKNOWLEDGMENTS

We are grateful to Drs. Daniel Herschlag and Patrick Brown (Department of Biochemistry, Stanford University) for their help in initiating this project. We also thank Drs. Kelly Shepard and Ron Vale (University of California at San Francisco) for providing plasmids carrying U1A-tagged bud-localized genes, Dr. Toshifumi Inada (Nagoya University, Japan) and Dr. Mitsuru Okuwaki

(University of Tsukuba, Japan) for valuable discussions, and Dr. Kunihiro Matsumoto (Nagoya University, Japan) for critical reading of this manuscript. A.P.G. is supported by a Career Development Award from the International Human Frontier Science Program Organization (HFSP). K.I. is supported by grants-in-aid for Scientific Research from the Ministry of Education, Science, Sports, Culture, and Technology, Japan (2005–2007) and by a grant from Kato Memorial Bioscience Foundation.

Received January 25, 2008; accepted August 4, 2008.

REFERENCES

Andoh, T., Oshiro, Y., Hayashi, S., Takeo, H., and Tani, T. 2006. Visual screening for localized RNAs in yeast revealed novel RNAs at the bud-tip. *Biochem. Biophys. Res. Commun.* **351:** 999–1004.

Bailey, T.L. and Elkan, C. 1994. Fitting a mixture model by expectation maximization to discover motifs in biopolymers. *Proceedings of the Second International Conference on Intelligent Systems for Molecular Biology.* pp 28–36. AAAI Press, Stanford, CA; Menlo Park, CA.

Baudin, A., Ozier, K.O., Denouel, A., Lacroute, F., and Cullin, C. 1993. A simple and efficient method for direct gene deletion in *Saccharomyces cerevisiae*. *Nucleic Acids Res.* **21:** 3329–3330.

Berglund, J.A., Chua, K., Abovich, N., Reed, R., and Rosbash, M. 1997. The splicing factor BBP interacts specifically with the pre-mRNA branchpoint sequence UACUAAC. *Cell* **89:** 781–787.

Bertrand, E., Chartrand, P., Schaefer, M., Shenoy, S.M., Singer, R.H., and Long, R.M. 1998. Localization of *ASH1* mRNA particles in living yeast. *Mol. Cell* **2:** 437–445.

Bobola, N., Jansen, R.P., Shin, T.H., and Nasmyth, K. 1996. Asymmetric accumulation of Ash1p in postanaphase nuclei depends on a myosin and restricts yeast mating-type switching to mother cells. *Cell* **84:** 699–709.

Bohl, F., Kruse, C., Frank, A., Ferring, D., and Jansen, R.P. 2000. She2p, a novel RNA-binding protein tethers *ASH1* mRNA to the Myo4p myosin motor via She3p. *EMBO J.* **19:** 5514–5524.

Bomsztyk, K., Denisenko, O., and Ostrowski, J. 2004. hnRNP K: One protein multiple processes. *Bioessays* **26:** 629–638.

Buckanovich, R.J. and Darnell, R.B. 1997. The neuronal RNA binding protein Nova-1 recognizes specific RNA targets in vitro and in vivo. *Mol. Cell. Biol.* **17:** 3194–3201.

Chartrand, P., Meng, X.H., Singer, R.H., and Long, R.M. 1999. Structural elements required for the localization of *ASH1* mRNA and of a green fluorescent protein reporter particle in vivo. *Curr. Biol.* **9:** 333–336.

Czaplinski, K. and Singer, R.H. 2006. Pathways for mRNA localization in the cytoplasm. *Trends Biochem. Sci.* **31:** 687–693.

Demeter, J., Beauheim, C., Gollub, J., Hernandez-Boussard, T., Jin, H., Maier, D., Matese, J.C., Nitzberg, M., Wymore, F., Zachariah, Z.K., et al. 2007. The Stanford Microarray Database: Implementation of new analysis tools and open source release of software. *Nucleic Acids Res.* **35:** D766–D770.

Denisenko, O. and Bomsztyk, K. 2002. Yeast hnRNP K-like genes are involved in regulation of the telomeric position effect and telomere length. *Mol. Cell. Biol.* **22:** 286–297.

Diehn, M., Eisen, M.B., Botstein, D., and Brown, P.O. 2000. Large-scale identification of secreted and membrane-associated gene products using DNA microarrays. *Nat. Genet.* **25:** 58–62.

Du, T.G., Schmid, M., and Jansen, R.P. 2007. Why cells move messages: The biological functions of mRNA localization. *Semin. Cell Dev. Biol.* **18:** 171–177.

Evangelista, M., Blundell, K., Longtine, M.S., Chow, C.J., Adames, N., Pringle, J.R., Peter, M., and Boone, C. 1997. Bni1p, a yeast formin linking cdc42p and the actin cytoskeleton during polarized morphogenesis. *Science* **276:** 118–122.

Gerber, A.P., Herschlag, D., and Brown, P.O. 2004. Extensive association of functionally and cytotopically related mRNAs with Puf family RNA-binding proteins in yeast. *PLoS Biol.* **2:** 342–354.

Gerber, A.P., Luschnig, S., Krasnow, M.A., Brown, P.O., and Herschlag, D. 2006. Genome-wide identification of mRNAs associated with the translational regulator PUMILIO in *Drosophila melanogaster*. *Proc. Natl. Acad. Sci.* **103:** 4487–4492.

Ghaemmaghami, S., Huh, W.K., Bower, K., Howson, R.W., Belle, A., Dephoure, N., O'Shea, E.K., and Weissman, J.S. 2003. Global analysis of protein expression in yeast. *Nature* **425:** 737–741.

Gonzalez, I., Buonomo, S.B., Nasmyth, K., and von Ahsen, U. 1999. *ASH1* mRNA localization in yeast involves multiple secondary structural elements and Ash1 protein translation. *Curr. Biol.* **9:** 337–340.

Gonsalvez, G.B., Urbinati, C.R., and Long, R.M. 2005. RNA localization in yeast: Moving towards a mechanism. *Biol. Cell.* **97:** 75–86.

Gu, W., Deng, Y., Zenklusen, D., and Singer, R.H. 2004. A new yeast PUF family protein, Puf6p, represses ASH1 mRNA translation and is required for its localization. *Genes & Dev.* **18:** 1452–1465.

Haarer, B.K., Petzold, A., Lillie, S.H., and Brown, S.S. 1994. Identification of *MYO4*, a second class V myosin gene in yeast. *J. Cell Sci.* **107:** 1055–1064.

Halbeisen, R.E., Galgano, A., Scherrer, T., and Gerber, A.P. 2008. Post-transcriptional gene regulation: From genome-wide studies to principles. *Cell. Mol. Life Sci.* **65:** 798–813.

Hieronymus, H., Yu, M.C., and Silver, P.A. 2004. Genome-wide mRNA surveillance is coupled to mRNA export. *Genes & Dev.* **18:** 2652–2662.

Holcik, M. and Liebhaber, S.A. 1997. Four highly stable eukaryotic mRNAs assemble 3′ untranslated region RNA-protein complexes sharing cis and trans components. *Proc. Natl. Acad. Sci.* **94:** 2410–2414.

Holstege, F.C., Jennings, E.G., Wyrick, J.J., Lee, T.I., Hengartner, C.J., Green, M.R., Golub, T.R., Lander, E.S., and Young, R.A. 1998. Dissecting the regulatory circuitry of a eukaryotic genome. *Cell* **95:** 717–728.

Huxley, C., Green, E.D., and Dunham, I. 1990. Rapid assessment of *S. cerevisiae* mating type by PCR. *Trends Genet.* **6:** 236.

Inada, T. and Aiba, H. 2005. Translation of aberrant mRNAs lacking a termination codon or with a shortened 3′-UTR is repressed after initiation in yeast. *EMBO J.* **24:** 1584–1595.

Irie, K., Tadauchi, T., Takizawa, P.A., Vale, R.D., Matsumoto, K., and Herskowitz, I. 2002. The Khd1 protein, which has three KH RNA-binding motifs, is required for proper localization of *ASH1* mRNA in yeast. *EMBO J.* **21:** 1158–1167.

Jambhekar, A., McDermott, K., Sorber, K., Shepard, K.A., Vale, R.D., Takizawa, P.A., and DeRisi, J.L. 2005. Unbiased selection of localization elements reveals *cis*-acting determinants of mRNA bud localization in *Saccharomyces cerevisiae*. *Proc. Natl. Acad. Sci.* **102:** 18005–18010.

Jansen, R.P., Dowzer, C., Michaelis, C., Galova, M., and Nasmyth, K. 1996. Mother cell-specific *HO* expression in budding yeast depends on the unconventional myosin Myo4p and other cytoplasmic proteins. *Cell* **84:** 687–697.

Kaiser, C.A., Adams, A., and Gottschling, D.E. 1994. *Methods in yeast genetics*. Cold Spring Harbor Laboratory Press, Cold Spring Harbor, N.Y.

Kanamori, H., Dodson, R.E., and Shapiro, D.J. 1998. In vitro genetic analysis of the RNA binding site of vigilin, a multi-KH-domain protein. *Mol. Cell. Biol.* **18:** 3991–4003.

Keene, J.D. 2007. RNA regulons: Coordination of post-transcriptional events. *Nat. Rev. Genet.* **8:** 533–543.

Long, R.M., Singer, R.H., Meng, X., Gonzalez, I., Nasmyth, K., and Jansen, R.P. 1997. Mating type switching in yeast controlled by asymmetric localization of *ASH1* mRNA. *Science* **277:** 383–387.

Long, R.M., Gu, W., Lorimer, E., Singer, R.H., and Chartrand, P. 2000. She2p is a novel RNA-binding protein that recruits the Myo4p-She3p complex to *ASH1* mRNA. *EMBO J.* **19:** 6592–6601.

Long, R.M., Gu, W., Meng, X., Gonsalvez, G., Singer, R.H., and Chartrand, P. 2001. An exclusively nuclear RNA-binding protein affects asymmetric localization of *ASH1* mRNA and Ash1p in yeast. *J. Cell Biol.* **153:** 307–318.

Longtine, M.S., McKenzie, A.R., Demarini, D.J., Shah, N.G., Wach, A., Brachat, A., Philippsen, P., and Pringle, J.R. 1998. Additional modules for versatile and economical PCR-based gene deletion and modification in *Saccharomyces cerevisiae*. *Yeast* **14:** 953–961.

López de Heredia, M. and Jansen, R.P. 2004. mRNA localization and the cytoskeleton. *Curr. Opin. Cell Biol.* **16:** 80–85.

Makeyev, A.V. and Liebhaber, S.A. 2002. The poly(C)-binding proteins: A multiplicity of functions and a search for mechanisms. *RNA* **8:** 265–278.

Müller, M., Heuck, A., and Niessing, D. 2007. Directional mRNA transport in eukaryotes: Lessons from yeast. *Cell. Mol. Life Sci.* **64:** 171–180.

Munchow, S., Sauter, C., and Jansen, R.P. 1999. Association of the class V myosin Myo4p with a localised messenger RNA in budding yeast depends on She proteins. *J. Cell Sci.* **112:** 1511–1518.

Musunuru, K. and Darnell, R.B. 2004. Determination and augmentation of RNA sequence specificity of the Nova K-homology domains. *Nucleic Acids Res.* **32:** 4852–4861.

Niessing, D., Hüttelmaier, S., Zenklusen, D., Singer, R.H., and Burley, S.K. 2004. She2p is a novel RNA binding protein with a basic helical hairpin motif. *Cell* **119:** 491–502.

Olivier, C., Poirier, G., Gendron, P., Boisgontier, A., Major, F., and Chartrand, P. 2005. Identification of a conserved RNA motif essential for She2p recognition and mRNA localization to the yeast bud. *Mol. Cell. Biol.* **25:** 4752–4766.

Ostareck, D.H., Ostareck-Lederer, A., Wilm, M., Thiele, B.J., Mann, M., and Hentze, M.W. 1997. mRNA silencing in erythroid differentiation: hnRNP K and hnRNP E1 regulate 15-lipoxygenase translation from the 3′ end. *Cell* **89:** 597–606.

Paquin, N., Ménade, M., Poirier, G., Donato, D., Drouet, E., and Chartrand, P. 2007. Local activation of yeast ASH1 mRNA translation through phosphorylation of Khd1p by the casein kinase Yck1p. *Mol. Cell* **26:** 795–809.

Parker, R. and Sheth, U. 2007. P bodies and the control of mRNA translation and degradation. *Mol. Cell* **25:** 635–646.

Parsons, A.B., Lopez, A., Givoni, I.E., Williams, D.E., Gray, C.A., Porter, J., Chua, G., Sopko, R., Brost, R.L., Ho, C.H., et al. 2006. Exploring the mode-of-action of bioactive compounds by chemical-genetic profiling in yeast. *Cell* **126:** 611–625.

Paziewska, A., Wyrwicz, L.S., and Ostrowski, J. 2005. The binding activity of yeast RNAs to yeast Hek2p and mammalian hnRNP K proteins, determined using the three-hybrid system. *Cell. Mol. Biol. Lett.* **10:** 227–235.

Rajavel, M., Philip, B., Buehrer, B.M., Errede, B., and Levin, D.E. 1999. Mid2 is a putative sensor for cell integrity signaling in *Saccharomyces cerevisiae*. *Mol. Cell. Biol.* **19:** 3969–3976.

Rigaut, G., Shevchenko, A., Rutz, B., Wilm, M., Mann, M., and Séraphin, B. 1999. A generic protein purification method for protein complex characterization and proteome exploration. *Nat. Biotechnol.* **17:** 1030–1032.

Ross, A.F., Oleynikov, Y., Kislauskis, E.H., Taneja, K.L., and Singer, R.H. 1997. Characterization of a β-actin mRNA zipcode-binding protein. *Mol. Cell. Biol.* **17:** 2158–2165.

Sakumoto, N., Mukai, Y., Uchida, K., Kouchi, T., Kuwajima, J., Nakagawa, Y., Sugioka, S., Yamamoto, E., Furuyama, T., Mizubuchi, H., et al. 1999. A series of protein phosphatase gene disruptants in *Saccharomyces cerevisiae*. *Yeast* **15:** 1669–1679.

Sambrook, J., Fritsch, E.F., and Maniatis, T. 1989. *Molecular cloning: A laboratory manual*, 2nd ed. Cold Spring Harbor Laboratory Press, Cold Spring Harbor, N.Y.

Schmid, M., Jaedicke, A., Du, T.G., and Jansen, R.P. 2006. Coordination of endoplasmic reticulum and mRNA localization to the yeast bud. *Curr. Biol.* **16:** 1538–1542.

Schneider, B.L., Steiner, B., Seufert, W., and Futcher, A.B. 1996. pMPY-ZAP: A reusable polymerase chain reaction-directed gene disruption cassette for *Saccharomyces cerevisiae*. *Yeast* **12:** 129–134.

Shepard, K.A., Gerber, A.P., Jambhekar, A., Takizawa, P.A., Brown, P.O., Herschlag, D., DeRisi, J.L., and Vale, R.D. 2003. Widespread cytoplasmic mRNA transport in yeast: Identification of 22 bud-localized transcripts using DNA microarray analysis. *Proc. Natl. Acad. Sci.* **100:** 11429–11434.

Sikorski, R.S. and Hieter, P. 1989. A system of shuttle vectors and yeast host strains designed for efficient manipulation of DNA in *Saccharomyces cerevisiae*. *Genetics* **122:** 19–27.

Sil, A. and Herskowitz, I. 1996. Identification of asymmetrically localized determinant, Ash1p, required for lineage-specific transcription of the yeast *HO* gene. *Cell* **84:** 711–722.

Siomi, H., Choi, M., Siomi, M.C., Nussbaum, R.L., and Dreyfuss, G. 1994. Essential role for KH domains in RNA binding: Impaired RNA binding by a mutation in the KH domain of FMR2 that causes fragile X symdrome. *Cell* **77:** 33–39.

St Johnston, D. 2005. Moving messages: The intracellular localization of mRNAs. *Nat. Rev. Mol. Cell Biol.* **6:** 363–375.

Tadauchi, T., Matsumoto, K., Herskowitz, I., and Irie, K. 2001. Post-transcriptional regulation through the *HO* 3′-UTR by Mpt5, a yeast homolog of Pumilio and FBF. *EMBO J.* **20:** 552–561.

Takizawa, P.A. and Vale, R.D. 2000. The myosin motor, Myo4p, binds Ash1 mRNA via the adapter protein, She3p. *Proc. Natl. Acad. Sci.* **97:** 5273–5278.

Takizawa, P.A., Sil, A., Swedlow, J.R., Herskowitz, I., and Vale, R.D. 1997. Actin-dependent localization of an RNA encoding a cell-fate determinant in yeast. *Nature* **389:** 90–93.

Takizawa, P.A., DeRisi, J.L., Wilhelm, J.E., and Vale, R.D. 2000. Plasma membrane compartmentalization in yeast by messenger RNA transport and a septin diffusion barrier. *Science* **290:** 341–344.

Tekotte, H. and Davis, I. 2002. Intracellular mRNA localization: Motors move messages. *Trends Genet.* **18:** 636–642.

Tusher, V.G., Tibshirani, R., and Chu, G. 2001. Significance analysis of microarrays applied to the ionizing radiation response. *Proc. Natl. Acad. Sci.* **98:** 5116–5121.

Wang, Y., Liu, C.L., Storey, J.D., Tibshirani, R.J., Herschlag, D., and Brown, P.O. 2002. Precision and functional specificity in mRNA decay. *Proc. Natl. Acad. Sci.* **99:** 5860–5865.

Wendland, B., McCaffery, J.M., Xiao, Q., and Emr, S.D. 1996. A novel fluorescence-activated cell sorter-based screen for yeast endocytosis mutants identifies a yeast homologue of mammalian eps15. *J. Cell Biol.* **135:** 1485–1500.

Wickens, M., Bernstein, D.S., Kimble, J., and Parker, R. 2002. A PUF family portrait: 3′-UTR regulation as a way of life. *Trends Genet.* **18:** 150–157.